 doi:10.20944/preprints202103.0655.v1

Article

ATPase inhibitor factor-1 disrupts mitochondrial Ca2+ handling and promotes pathological cardiac hypertrophy through CaMKIIδ

Mario G. Pavez-Giani[1], Pablo Sánchez Aguilera[1#], Nils Bomer[1#], Shigeki Miyamoto[2], Harmen G. Booij,[1] Paula Giraldo[1], Silke U. Oberdorf-Maass[1], Kirsten T. Nijholt[1], Salva R. Yurista[1], Hendrik Milting[3], Peter van der Meer[1], Rudolf A. de Boer[1], Joan Heller Brown[2], Herman W. H. Sillje[1], B. Daan Westenbrink[1*]

[1]Department of Cardiology, University Medical Center Groningen, University of Groningen, Groningen, The Netherlands.

[2] Department of Pharmacology, University of California San Diego, San Diego, CA, USA.

[3] Heart- und Diabetescenter NRW, University Hospital of the Ruhr University Bochum, Erich and Hanna Klessmann-Institute for Cardiovascular Research and Development, Bad Oeynhausen, Germany

* Correspondence: b.d.westenbrink@umcg.nl

 doi:10.20944/preprints202103.0655.v1

Abstract:

Background :

ATPase inhibitor factor-1 (IF1) preserves cellular ATP under conditions of respiratory collapse, yet the function of IF1 under normal respiring conditions is unresolved. We tested the hypothesis that IF1 promotes mitochondrial dysfunction and pathological cardiomyocyte hypertrophy in the context of heart failure (HF).

Methods and results

Cardiac expression of IF1 was increased in mice and in humans with HF, downstream of neurohumoral signaling pathways and in patterns that resembled the fetal-like gene program. Adenoviral expression of wild type IF1 in primary cardiomyocytes resulted in pathological hypertrophy and metabolic remodeling as evidenced by enhanced mitochondrial oxidative stress, reduced mitochondrial respiratory capacity, and the augmentation of extra-mitochondrial glycolysis. Similar perturbations were observed with an IF1 mutant incapable of binding to ATP-synthase (E55A mutation), indication that these effects occurred independent of binding to ATP synthase. Instead, IF1 promoted mitochondrial fragmentation and compromised mitochondrial Ca2+ handling, which resulted in sarcoplasmic reticulum Ca2+ overloading. The effects of IF1 on Ca2+ handling were associated with the cytosolic activation of CaMKII and inhibition of CaMKII or co-expression of catalytically dead CaMKIIδC was sufficient to prevent IF-1 induced pathological hypertrophy.

Conclusions

IF1 represents a novel member of the fetal-like gene program that contributes to mitochondrial dysfunction and pathological cardiac remodeling in HF. Furthermore, we present evidence for a novel, ATP-synthase independent, role for IF1 in mitochondrial Ca2+ handling and mitochondrial- to nuclear crosstalk involving CaMKII.

Keywords: mitochondria; calcium handling; heart failure; CaMKII; cardiomyocyte hypertrophy

Introduction

The heart requires tremendous amounts of ATP to sustain the systemic circulation, most of which is generated by mitochondria. In patients with HF, metabolic roadblocks and structural damage to mitochondria occur that induce

 doi:10.20944/preprints202103.0655.v1

mitochondrial oxidative stress and diminishing myocardial ATP production[1]. It has become increasingly clear that "retrograde" signals originating from dysfunctional mitochondria activate nuclear gene transcription that promotes maladaptive cardiac growth[2]. Enhanced understanding of pathways underlying these retrograde mitochondrial- to nuclear crosstalk in HF could uncover new treatments for HF patients.

ATP synthase is a reversible rotary enzyme that synthesizes ATP when driven by a mitochondrial membrane potential ($\Delta\psi_m$) that is generated by the respiratory chain[3]. When the $\Delta\psi_m$ dissipates, under ischemic conditions or in critically damaged mitochondria, ATP-synthase reverses its direction of rotation and becomes an ATP consumer rather than a generator. Reversal of ATP-synthase is specifically blocked by the evolutionary conserved mitochondrial protein ATPase inhibitory factor 1 (IF1 or ATPIF1)[4]. By blocking ATP synthase reversal, IF1 conserves ATP and permits eradication of depolarized dysfunctional mitochondria; thereby preserving cellular viability under ischemic conditions[5].

It has long been thought that the biological function of IF1 was restricted to conditions of respiratory collapse. Recent studies have, however, uncovered a number of physiological roles for IF1 under respiring conditions, including but not restricted to the regulation of mitochondrial oxidative stress[6], Ca2+ handling[7], cristae formation[8,9], glucose metabolism[10,11], and neuronal development[12,13]. While the role of binding to ATP synthase in these processes is disputed, there is general consensus that many of these non-canonical roles of IF1 are governed by mitochondrial- to nuclear signaling[6,7,10,11,14]. While relatively little is known about the role of IF1 in HF, Yang *et al.* were recently the first to demonstrated that IF1 is upregulated in HF and that IF1 knock out mice are less susceptible to pressure overload-induced HF[14]. Based on the above, we hypothesized that IF1 is a critical regulator of mitochondrial-nuclear crosstalk that combines mitochondrial dysfunction and maladaptive cardiomyocyte remodeling in HF.

In the present study we present evidence supporting a key role for IF1 in mitochondrial reprograming and maladaptive cardiac remodeling in cardiomyocytes that is independent of its interaction with ATP synthase. Instead, we uncovered a novel and translationally relevant pathway that positions IF1 at the intersection of mitochondrial Ca2+ handling and mitochondrial- to nuclear crosstalk in cardiomyocytes. By doing so, we provide direct evidence for a physiological role for IF1 that is truly independent of ATP synthase.

 doi:10.20944/preprints202103.0655.v1

Results

Myocardial expression of IF-1 is increased in heart failure and induces metabolic reprogramming in NRVM

To corroborate previous reports that indicated that the expression of IF1 is increased in failing hearts [14], IF1 mRNA expression was determined in the LV lysates obtained from several models of murine HF: mice with cardiomyocyte autonomous expression of activated Gαq [15], mice subjected to transverse aortic constriction (TAC) [20], or mice subjected to a myocardial infarction (MI) [16]. In all 3 models, IF1 expression levels were increased by 3-fold compared to control mice (**Figure 1A**). The increased mRNA expression of IF1 corresponded with a similar increase in IF1 protein levels (**Figure S1A**). IF-1 mRNA levels were also higher in cardiac lysates obtained from patients with end stage HF compared to control hearts (**Figure 1B**). In Neonatal Rat Ventricular Cardiomyocytes (NRVM), overexpression of Gαq (**Figure S1B**) and treatment with isoproterenol (**Figure 1C**) which both stimulate pathological hypertrophy resulted in a significant increase in the expression of IF-1. In contrast, treatment with insulin like growth factor-1 (IGF-1) which stimulates physiological cardiac growth did not affect IF-1 expression levels (**Figure 1C**). The expression of IF1 increased during consecutive stages of embryonic development, to reduce after birth (**Figure S1C)**. IF-1 expression increased again in mice with HF. Together these findings suggest that IF1 is regulated downstream of maladaptive neurohumoral signaling pathways in patterns mimicking the fetal-like gene program.

Preprints (www.preprints.org) | NOT PEER-REVIEWED | Posted: 26 March 2021 doi:10.20944/preprints202103.0655.v1

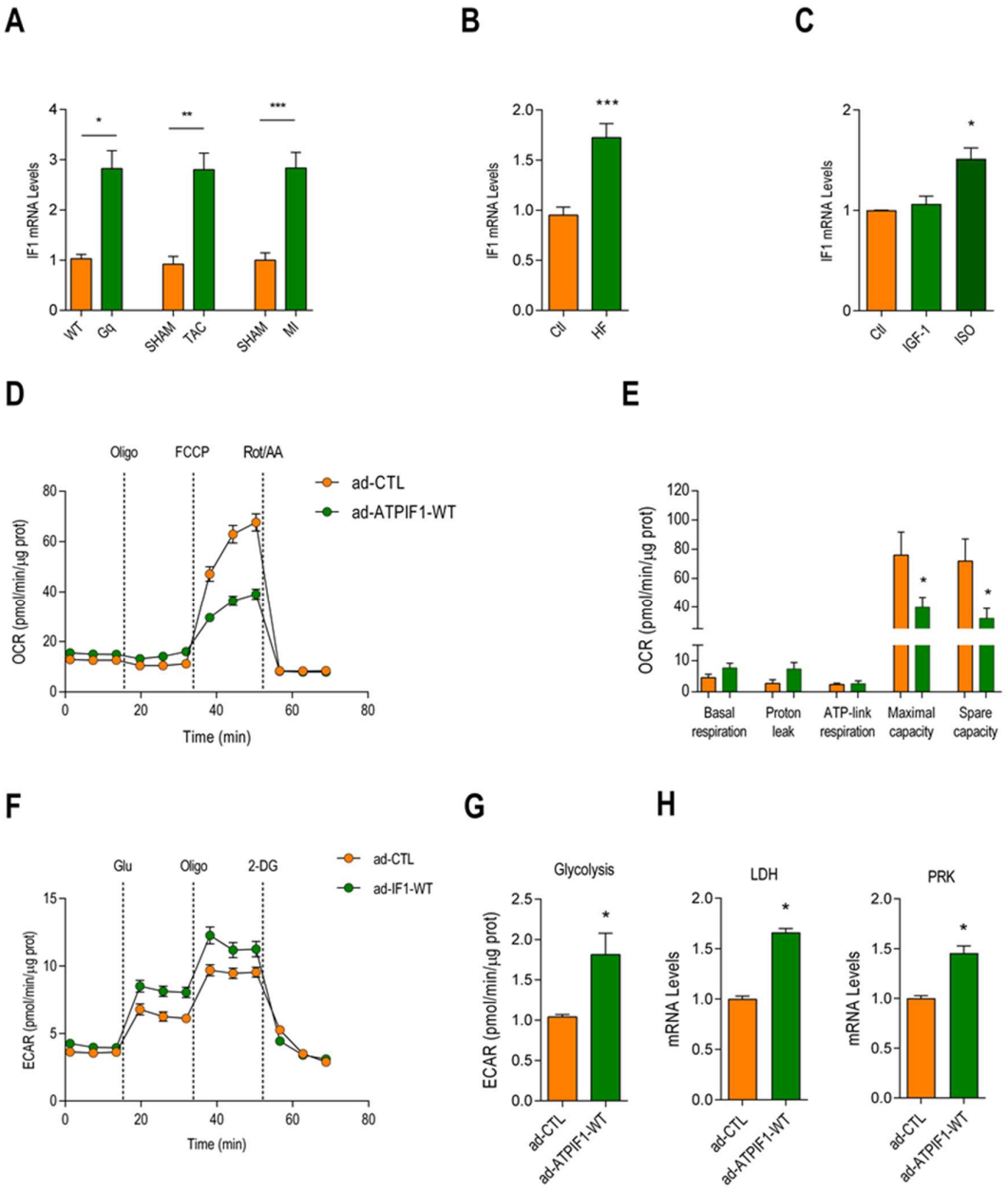

Figure 1. Expression of IF1 is increased in Heart Failure, decreases mitochondrial respiratory capacity, and promotes glycolysis in cardiomyocytes. ***(A)*** *IF-1 mRNA levels in mice with heart failure induced by cardiomyocyte autonomous expression of Gαq (Gq) and wild type (WT) littermate controls (n=4), mice with heart failure induced by Transverse Aortic Constriction (TAC) (n=6) or Myocardial Infarction (MI) (n=6) surgeries and SHAM operated controls (both n=6).* ***(B)*** *mRNA expression of IF-1 in cardiac lysates from patients with end stage heart failure and normal control hearts (n=11).* ***(C)*** *IF-1 mRNA expression in NRVM treated with Insulin-like Growth Factor-1 (IGF-1, 10 nM), Isoproterenol (ISO, 100 nM) or vehicle (Ctl) for 48 hr (n=4).* ***(D)*** *Neonatal rat ventricular myocytes (NRVM) were infected with an adenoviral vector expressing*

Preprints (www.preprints.org) | NOT PEER-REVIEWED | Posted: 26 March 2021 doi:10.20944/preprints202103.0655.v1

human IF1 (ad-IF1-WT), or a control virus expressing GFP (ad-CTL) for 48 hrs. The line graph depicts changes in oxygen consumption rate (OCR) of NRVM after serial treatments with oligomycin (oligo), FCCP and rot + AA assessed with the SeaHorse system. (n=5 independent experiments). ***(E)*** *Bar graph depicting differences in basal respiration, ATP-linked respiration, maximal respiration, and mitochondrial spare capacity (n=5).* ***(F)*** *Changes in extracellular acidification rate (ECAR) in cells infected with ad-IF1-WT or ad-CTL after serial additions of glucose, oligomycin and 2-deoxyglucose (2-DG, n=4)* ***(G)*** *Bar graph depicting differences in glycolysis in NRVM treated as in* ***F*** *(n=4).* ***(H)*** *mRNA levels of Lactate dehydrogenase (LDH) and Pyruvate kinase (PRK) assayed with RT-qPCR (n=4). Data are presented as mean ± SEM. *p < 0.05, **p < 0.01 and ***p < 0.001 vs ad-CTL by nonparametric Mann-Whitney test (C, G and H). Data are presented as mean ± SEM. * p < 0.05, ** p < 0.01 and *** p < 0.001 vs SHAM/Ctrl/ad-CTL using the ad-CTL using the Mann-Whitney U test or T-test where appropriate.*

To determine the consequences of increased expression of IF1 on mitochondrial function in cardiomyocytes, NRVM's were infected with an adenoviral vector expressing human IF1 (ad-IF1-WT), or a control virus expressing GFP (ad-CTL)[22]. Infection with ad-IF1-WT resulted in a 7-fold increase in the protein levels of IF1 (**Figure S2A**). As expected, the drop in mitochondrial membrane potential following respiratory collapse was increased by ad-IF1-WT (**Figure S2B-C**) and preserved intracellular ATP levels, consistent with stronger inhibition of the reverse mode of ATPsynthase (**Figure S2D**). Infection with IF1 did not affect cellular viability for up to 2 days after infection (**Figure S2E**).

To determine the consequences of increased IF1 expression under respiring conditions, mitochondrial oxygen consumption rate (OCR) was measured using a SeaHorse metabolic flux analyzer. Overexpression of IF-1 did not influence basal or ATP-linked respiration, nor did it affect the proton leak (**Figure 1D, E and S2F**). IF1 did, however, result in a dose dependent decrease in the maximal mitochondrial respiration and a consequent reduction in mitochondrial spare capacity (**Figure 1E and S2F**). Reducing IF1 expression levels with an adenovirus expressing siRNA-IF1 did not influence mitochondrial respiration, arguing against a direct effect of IF1 on respiratory complexes **(Figure S2G and S2H)**. Next, we determined the consequences of IF1 on extra-mitochondrial metabolism by measuring extracellular acidification rates as a proxy of anaerobic glycolysis [23]. Infection with Ad-WT-IF1 resulted in a significant increase in anaerobic glycolysis (**Figure 1F, G**), accompanied by increased expression of the key glycolytic enzymes lactate dehydrogenase and pyruvate kinase (**Figure 1H**). Together these findings suggest that IF1 compromises maximal mitochondrial respiration and promotes extramitochondrial glycolysis without affecting ATP-linked respiration.

 doi:10.20944/preprints202103.0655.v1

IF1 induces mitochondrial oxidative stress and stimulates cardiomyocyte hypertrophy

IF1 has been shown to both increases- or decrease mitochondrial ROS emissions depending on the cell type and experimental context [5, 9, 24]. We therefore hypothesized that the reductions in maximal mitochondrial respiration could be explained by mitochondrial oxidative stress and/or downregulation of mitochondrial respiratory complexes. Compared to Ad-CTL infected cells, infection with Ad-IF1-WT resulted in a 40% increase in fluorescence intensity of the mitochondrial-specific ROS indicator MitoSox (**Figure 2A**). Similar increases in the expression of the ROS-responsive genes NADPH oxidase 2 (NOX2), Nuclear receptor factor-2 (NRF2) and Heat shock protein-60 (HSP60) were observed (**Figure 2B**). ROS-mediated mitochondrial DNA damage was also increased by 50% in ad-IF1-WT infected cells (**Figure 2C**). The protein expression of four out of five respiratory chain complexes were significantly reduced in ad-IF1-WT infected cells (**Figure 2D**). The reductions in maximal mitochondrial respiration induced by IF1 are thus accompanied by mitochondrial oxidative stress and reductions in electron chain complexes.

Overexpression of IF1 also resulted in a marked increase in cardiomyocyte size, (**Figure 2E)** accompanied by increases in mRNA levels atrial natriuretic peptide (ANP) and B-type natriuretic peptide (BNP) **(Figure 2F)**. The increases in cell size and natriuretic peptides were equivalent to those of 50 μM of phenylephrine (**Figure S3A and S3B**). The combination of phenylephrine and ad-WT-IF1 did not result in further increase in cell size or ANP. (**Figure S3A and S3B**). IF1 expression thus appears to be sufficient to promote pathological cardiomyocyte hypertrophy.

Preprints (www.preprints.org) | NOT PEER-REVIEWED | Posted: 26 March 2021 doi:10.20944/preprints202103.0655.v1

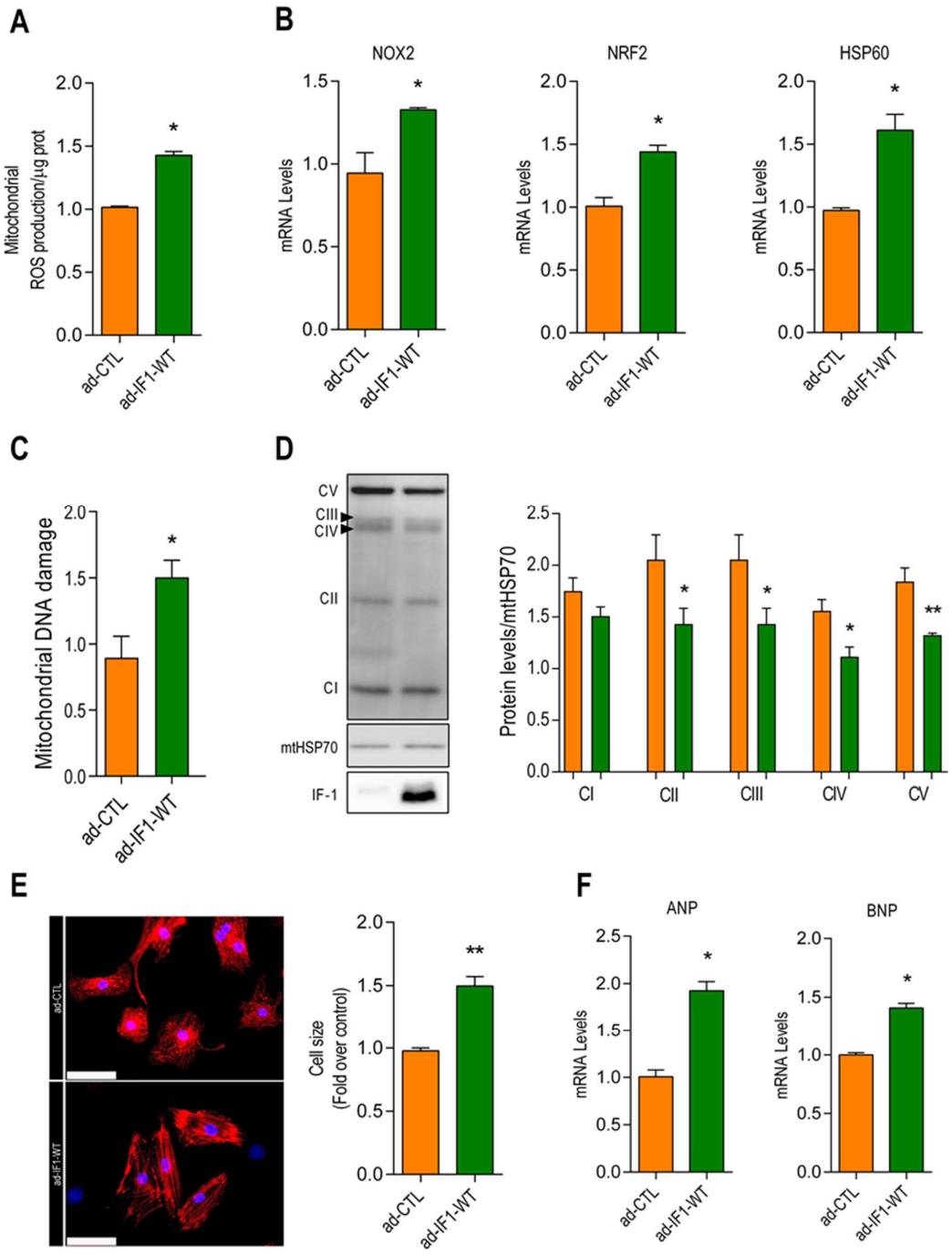

Figure 2. IF-1 overexpression promotes mitochondrial ROS production and cardiomyocyte hypertrophy. *NRVM were infected with an adenoviral vector expressing the human IF1 (ad-IF1-WT), or a control virus (ad-CTL) for 48 hrs.* ***(A)*** *Basal mitochondrial ROS emissions detected with the mitochondrial ROS sensor MitoSOX® (n=4).* ***(B)*** *mRNA expression of the mitochondrial ROS-sensitive genes NADPH oxidase 2 (NOX-2), Nuclear receptor factor-2 (NRF-2) and Heat shock protein-60 (HSP-60) (n=4).* ***(C)*** *Semi-log-run polymerase chain reaction was performed using specific primers for mitochondrial DNA*

Preprints (www.preprints.org) | NOT PEER-REVIEWED | Posted: 26 March 2021 doi:10.20944/preprints202103.0655.v1

fragments in the mitochondrial D-Loop region to determine oxidative damage to mitochondrial DNA (n=4). ***(D)*** *Changes in the protein levels of mitochondrial respiratory chain complexes in cells infected with ad-IF1-WT and ad-CTL detected by western blot and normalized for mitochondrial loading control heat shock protein-70 (mtHSP-70) levels. (n=4)* ***(E)*** *Typical example of immunofluorescent staining of NRVMs cultured with a fluorescent labelled anti-α-actinin (red, left panel) and (right panel) average cardiomyocyte surface area of α-actinin positive cells (n=5).* ***(F)*** *mRNA expression of atrial natriuretic peptide (ANP) and B-type natriuretic peptide (BNP) (n=5). Data are presented as mean ± SEM. *p < 0.05 and **p < 0.01 vs ad-CTL using the Mann-Whitney U test or T-test where appropriate.*

IF1-induced cardiomyocyte reprograming occurs independent of binding to ATP-synthase

To determine whether the effects of IF1 observed in our model were dependent on the interaction between IF1 to ATP synthase, part of the experiments in fig 1 and 2 were repeated with an adenovirus expressing a mutant form of IF1 in which glutamic acid 55 had been replaced by alanine (ad-IF1-E55A). This mutation renders IF1 incapable of binding to ATP-synthase [18].

Infection with ad-IF1-E55A resulted in similar increases in IF1 expression compared to ad-IF1-WT (**Figure S4A).** As expected, the drop in mitochondrial membrane potential following respiratory collapse was reduced by ad-IF1-E55A, consistent with diminished inhibition of the reverse mode of ATP-synthase (**Figure S4B**). Despite its inability to bind to ATP-synthase, infection with ad-IF1-E55A resulted in similar reductions in maximal mitochondrial respiration and mitochondrial spare capacity as did WT-IF1 (**Figure 3A** and **3B**). Infection with ad-IF1-E55A also resulted in a marked increase in glycolysis **(Figure 3C** and **3D**) as well as increased expression of LDH and PDK (**Figure 3E**). Mitochondrial ROS emissions were also increased after infection with ad-IF1-E55A (**Figure 3F**), as were the expression levels of NOX2, NRF2 and HSP60 (**Figure 3G**). Moreover, downregulation of the respiratory chain complexes II, IV and V was also observed with ad-IF1-E55A (**Figure S4C**). Finally, infection with ad-IF1-E55A induced cardiomyocyte hypertrophy that was proportional to what had been observed with Ad-IF1-WT (**Figure 3H)** and ANP and BNP mRNA expression were also significantly increased (**Figure S4D**). Together these data demonstrate that the effects of IF1 on mitochondrial function and cardiomyocyte hypertrophy are independent of binding of IF1 to ATP-synthase.

Preprints (www.preprints.org) | NOT PEER-REVIEWED | Posted: 26 March 2021 doi:10.20944/preprints202103.0655.v1

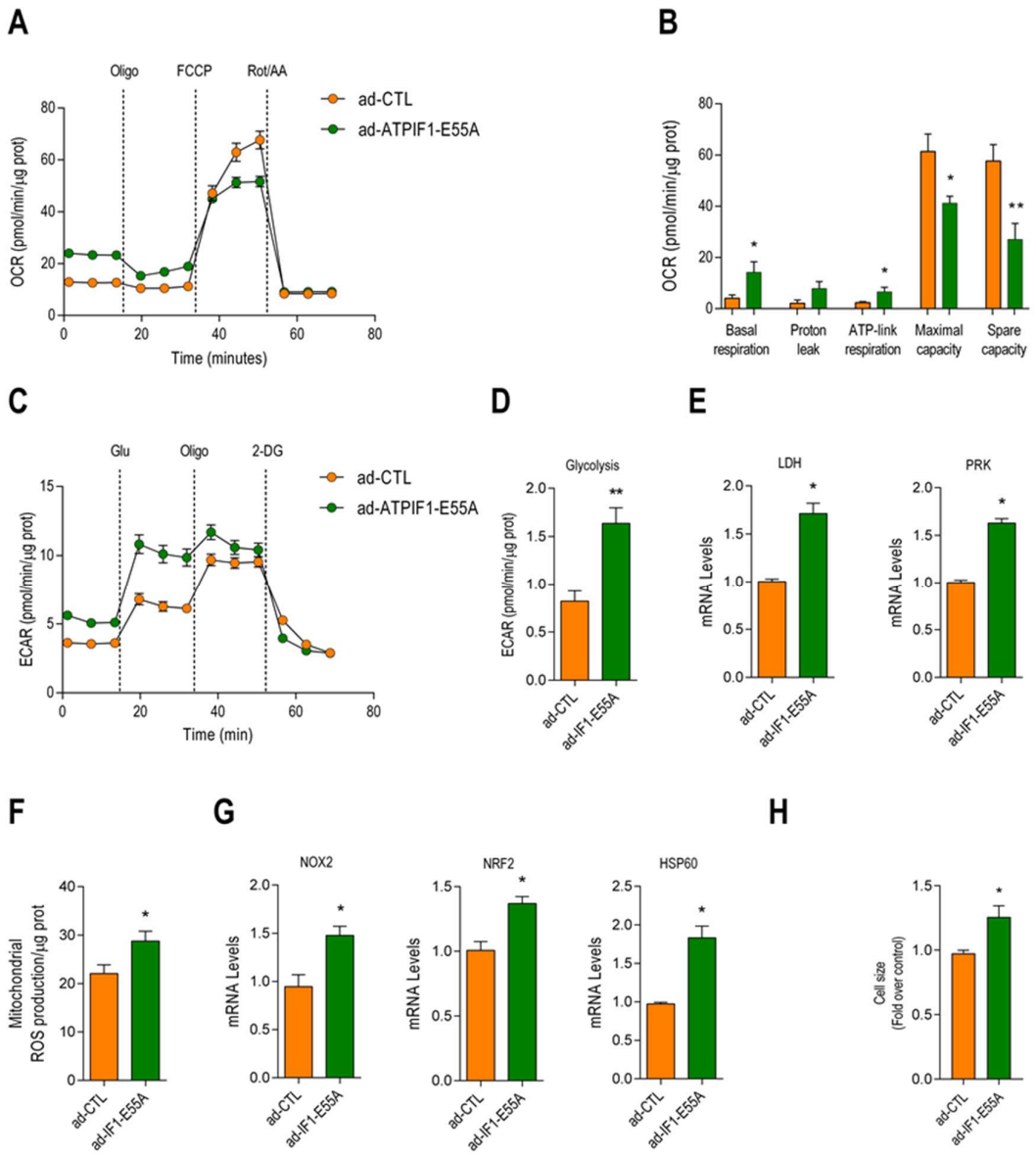

Figure 3. An IF-1 mutant incapable of binding to ATP-synthase induces similar degrees of mitochondrial stress and cardiomyocyte hypertrophy. *NRVMs were infected with and adenovirus expressing an IF1 mutant harbouring an E55A substitution that renders the protein unable to interact with ATP synthase or control virus (ad-CTL) for 48 hrs.* ***(A)*** *Changes in oxygen consumption rate (OCR) of NRVM after serial treatments with oligomycin (oligo), FCCP and rot + AA was assessed with the SeaHorse system. (n=5).* ***(B)*** *Bar graph depicting differences in basal respiration, ATP-linked respiration, maximal respiration and mitochondrial spare capacity (n=5).* ***(C)*** *Changes in extracellular acidification rate (ECAR) in cells infected with ad-IF1-E55A or ad-CTL after serial additions of glucose, oligomycin and 2-deoxyglucose (2-DG, n=4)* ***(D)*** *Bar graph depicting differences in glycolysis in NRVM treated as in* ***F*** *(n=4).* ***(E)*** *mRNA levels of Lactate dehydrogenase (LDH) and*

Preprints (www.preprints.org) | NOT PEER-REVIEWED | Posted: 26 March 2021 doi:10.20944/preprints202103.0655.v1

Pyruvate kinase (PRK) (n=5). ***(F)*** *Basal mitochondrial ROS levels assayed with MitoSOX® (n=4).* ***(G)*** *mRNA levels of NOX-2, NRF-2 and HSP-60.* ***(H)*** *Bar graph depicting differences in cardiomyocyte crossectional area (n=5). Data are presented as mean ± SEM. *p < 0.05 and **p < 0.01 vs ad-CTL using the Mann-Whitney U test or T-test where appropriate.*

IF-1 induces mitochondrial fission through DRP1

Altered mitochondrial dynamics are thought to contribute to mitochondrial dysfunction in heart failure [25-27]. Because IF1 has been implicated in the regulation of mitochondrial dynamics [6, 7, 34], we determined mitochondrial volume and morphology using confocal Z/y scanning followed by image deconvolution and 3D reconstruction. Typical examples of confocal images and multislice 3D reconstructions are depicted in **figure 4A and 4B**. Total mitochondrial volume and mitochondrial DNA copy numbers were not affected by IF1(**Figure S5A and S5B**). Infection with Ad-IF1-WT did, however, increase the number of mitochondria per cell and reduced the average mitochondrial volume and increased the fission index (**Figure 4C**), indicating that IF1 promotes mitochondrial fission in NRVC. A key step in the activation of mitochondrial fission is the phosphorylation and translocation of the GTPase protein called Dynamin-related protein 1 (DRP-1) to the outer mitochondrial membrane [28]. Infection with IF1 resulted in a marked increase in the mitochondrial translocation of DRP1 (**Figure 4D and E**). The myocardial expression of mitofusin-2 was decreased by IF1 (**Figure 4F and G**). Mitophagic flux was not affected under the current conditions as we did not observe mitochondrial translocation of Parkin or changes in the protein level of PINK1 (**Figure 4D-G**). In summary, we demonstrate that IF1 overexpression promotes mitochondrial fission without increasing mitophagic flux.

Preprints (www.preprints.org) | NOT PEER-REVIEWED | Posted: 26 March 2021 doi:10.20944/preprints202103.0655.v1

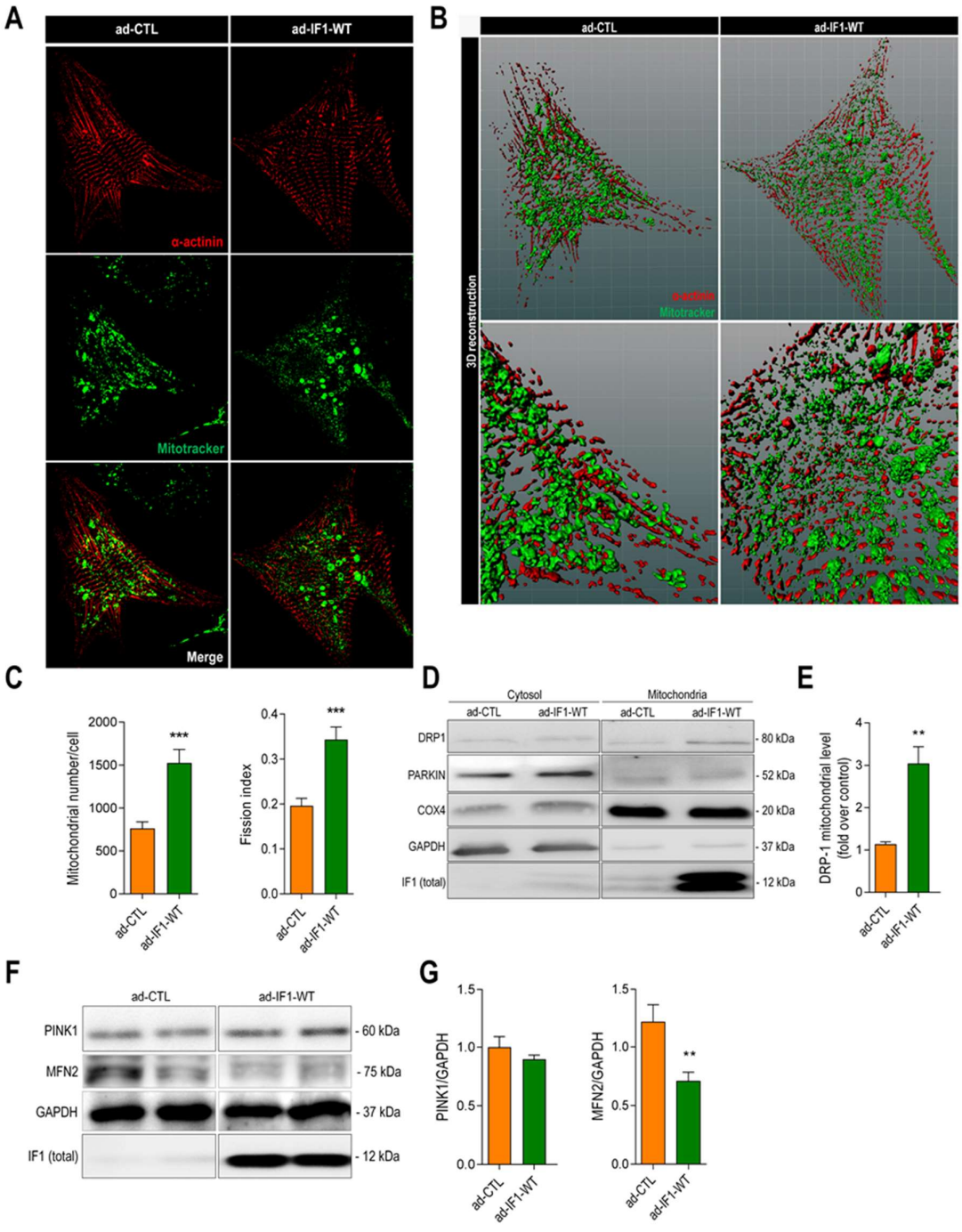

Preprints (www.preprints.org) | NOT PEER-REVIEWED | Posted: 26 March 2021 doi:10.20944/preprints202103.0655.v1

Figure 4. IF-1 induces mitochondrial fission by promoting DRP-1 translocation. *NRVMs were infected with adenovirus ad-IF1-WT or empty vector (ad-CTL) for 48 hrs.* ***(A)*** *Representative Z-stack image of neonatal rat ventricular myocyte stained with Mitotracker® Deep Red (green) and anti-α-actinin (red) using confocal microscopy* ***(B)*** *3D imaging reconstruction was employed for mitochondrial networks analysis (30-36 Z-stacks slices were recorded per cell). Representative example of confocal stack acquisition followed by 3D reconstruction after image deconvolution of cells stained as in* ***A****.* ***(C)*** *Bar graph depicting changes in the total mitochondrial volume per NRVM. (ad-CTL; n=17 cells and ad-IF1-WT; n=18 cells).* ***(C)*** *Bar graphs depicting differences in mitochondrial number per cell and the fission index expressed as the number of mitochondria normalized for mitochondrial volume per cell (ad-CTL; n=17 cells and ad-IF1-WT; n=18 cells).* ***(D)*** *Dynamin-1-like protein (DRP-1), Cytochrome c oxidase subunit 4 (COXIV) and GAPDH protein levels in mitochondrial and cytosolic fractions of NRVM infected with IF1-WT and ad-CTL.* ***(E)*** *DRP-1 protein levels normalized for COXIV in the mitochondrial fraction (n=4).* ***(F)*** *PINK1 and Mitofusin-2 (MFN2) protein levels normalized for GAPDH* ***(G)*** *Bar graphs depict densitometric analysis from protein levels normalized using immunoblot. Data are presented as mean ± SEM. *p < 0.05, **p < 0.01 and ***p < 0.001 vs ad-CTL using the Mann-Whitney U test or T-test where appropriate.*

IF-1 reduces mitochondrial Ca^{2+} and induces sarcoplasmic reticulum Ca^{2+} overload

It has been well described that mitochondrial dysfunction in the context of cardiomyocyte hypertrophy is associated with reductions in mitochondrial Ca Ca^{+2} [26, 29] . Moreover, it has been proposed that this is related to excessive mitochondrial fission which diminished the mitochondrial capacity to store Ca Ca^{2+} [30]. To determine whether IF1 affects mitochondrial Ca^{2+} levels, we first measured mitochondrial Ca2+ content with the mitochondrial Ca^{2+} specific dye Rhod2-AM. Cells infected with Ad-IF1-WT demonstrated a significant reduction in Rhod2-AM fluorescence, consistent with reduced mitochondrial Ca^{2+} content (**Figure 5A**). To confirm these observations, we also quantified FCCP-induced mitochondrial Ca2+ release using the cytosolic Ca^{2+}-sensitive dye Fluo4-AM. Indeed, FCCP-induced mitochondrial Ca2+ release was also significantly lower in NRVM infected with Ad-IF1-WT than in those infected with Ad-CTL (**Figure 5B** and **5C**). To determine how the reductions in mitochondrial Ca^{2+} content affected Ca^{2+} concentrations in other cellular compartments, we also determined Ca^{2+} concentrations in the cytosol and the sarcoplasmic reticulum using the ratiometric high affinity Ca^{2+} selective fluorescence indicator Fura 2-AM. Overexpression of ad-IF1-WT did not affect basal cytosolic Ca^{2+} levels (**Figure 5D**). However, potassium chloride-induced sarcoplasmic Ca^{2+} release was significantly increased in cells infected with ad-IF1-WT compared to ad-Ctrl. (**Figure 5E** and **5F**). Next, we assessed the mRNA expression of a panel of genes involved in the regulation of mitochondrial Ca^{2+} handling. Interestingly, IF1 resulted in a significant increase in the

Preprints (www.preprints.org) | NOT PEER-REVIEWED | Posted: 26 March 2021 doi:10.20944/preprints202103.0655.v1

expression of the dominant-negative pore-forming subunit of the mitochondrial Ca^{2+} uniporter ß (MCUB, **Figure 5G**). In summary, IF1-induced mitochondrial fragmentation and upregulation of MCUB compromises mitochondrial Ca^{2+} handling and promotes SR Ca^{2+} overloading.

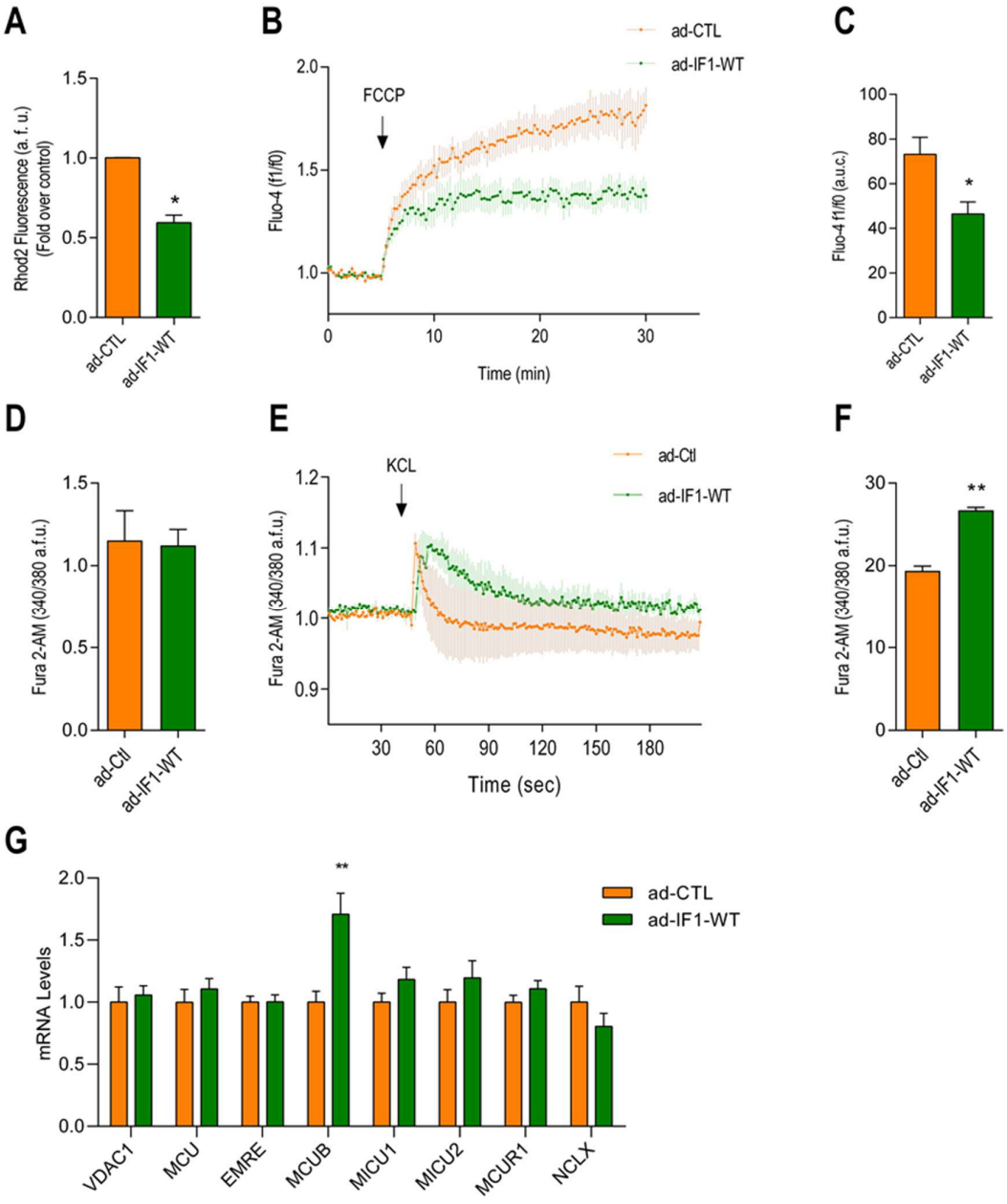

Figure 5. IF-1 reduces mitochondrial calcium, promotes SR-calcium overload, and activates CAMKII signaling. *NRVMs were infected with adenovirus ad-IF1-WT and ad-CTL for 48 hrs.* ***(A)*** *Bar graph depicting differences in basal mitochondrial Ca^{+2} detected by with Rhod-2 AM (n=4).* ***(B)*** *Time-lapse of mitochondrial Ca^{+2} release measurements using Fluo-4 AM before*

Preprints (www.preprints.org) | NOT PEER-REVIEWED | Posted: 26 March 2021 doi:10.20944/preprints202103.0655.v1

and after addition of FCCP (n=5). ***(C)*** *Differences in the area under the curve of Fluo-4 AM fluorescence after the addition of FCCP (n=5).* ***(D)*** *Cytosolic Ca^{+2} measurements using Fura-2 AM in cells infected with ad-IF1-WT or ad-CTL using an epifluorescence microscope (n=4).* ***(E)*** *Representative experiment of potassium chloride (KCL) induced sarcoplasmic reticulum (SR) Ca^{+2} release (n=3).* ***(F)*** *Bar graph depicting differences in the area under the curve of Fura-2 AM 340/380 fluorescence ratio after the addition of KCL (n=3).* ***(G)*** *Bar graphs depicting mRNA levels of different calcium regulatory genes assessed by qPCR; VDAC1, voltage dependent anion channel 1; MCU, mitochondrial calcium uniporter; EMRE, essential MCU regulatory element; MCUB, dominant-negative pore-forming subunit of the MCU ß; MICU, Mitochondrial calcium uptake protein; MCUR1 - MCU regulator 1; NCLX, mitochondrial sodium calcium exchanger (n=4). Data are presented as mean ± SEM. *p < 0.05, **p < 0.01 and ***p < 0.001 vs ad-CTL using the Mann-Whitney U test or T-test where appropriate.*

IF1 activates Ca^{+2}/calmodulin protein kinase II signaling

SR Ca^{2+} overloading can lead to the activation of Ca^{2+} and calmodulin sensitive signal transduction molecules, including Ca^{+2}/calmodulin protein kinase II (CaMKII) and calcineurin [31]. CaMKII and calcineurin both regulate pathological cardiac hypertrophy, suggesting that IF1-induced cardiomyocyte hypertrophy could be dependent on these pathways [32, 33]. To determine the effect of IF1 on CaMKII activation, we measured CaMKII autophosphorylation (Thr286) as well as the phosphorylation of the CaMKII-specific sites on its downstream targets Phospholamban (Thr17) and AMP-activated protein kinase (AMPK; Thr172). Infection with ad-IF1-WT resulted in CaMKII autophosphorylation and marked increases in the phosphorylation of its downstream targets (**Figure 6A and 6B**). Protein kinase-A dependent phosphorylation of CaMKII (Thr16) was not increased by IF1 (**Figure S6A**). No changes in the mRNA expression of Calcineurin response element 1 (RCAN1) were detected, indicating that calcineurin is not activated by IF1 (**Figure S6B**). Infection with ad-IF1-E55A had similar effects on mitochondrial Ca^{2+} handling and the activation of CaMKII-signaling (**Figure S7**), reinforcing the notion that these properties of IF1 are independent of its binding to ATP-synthase.

Preprints (www.preprints.org) | NOT PEER-REVIEWED | Posted: 26 March 2021 doi:10.20944/preprints202103.0655.v1

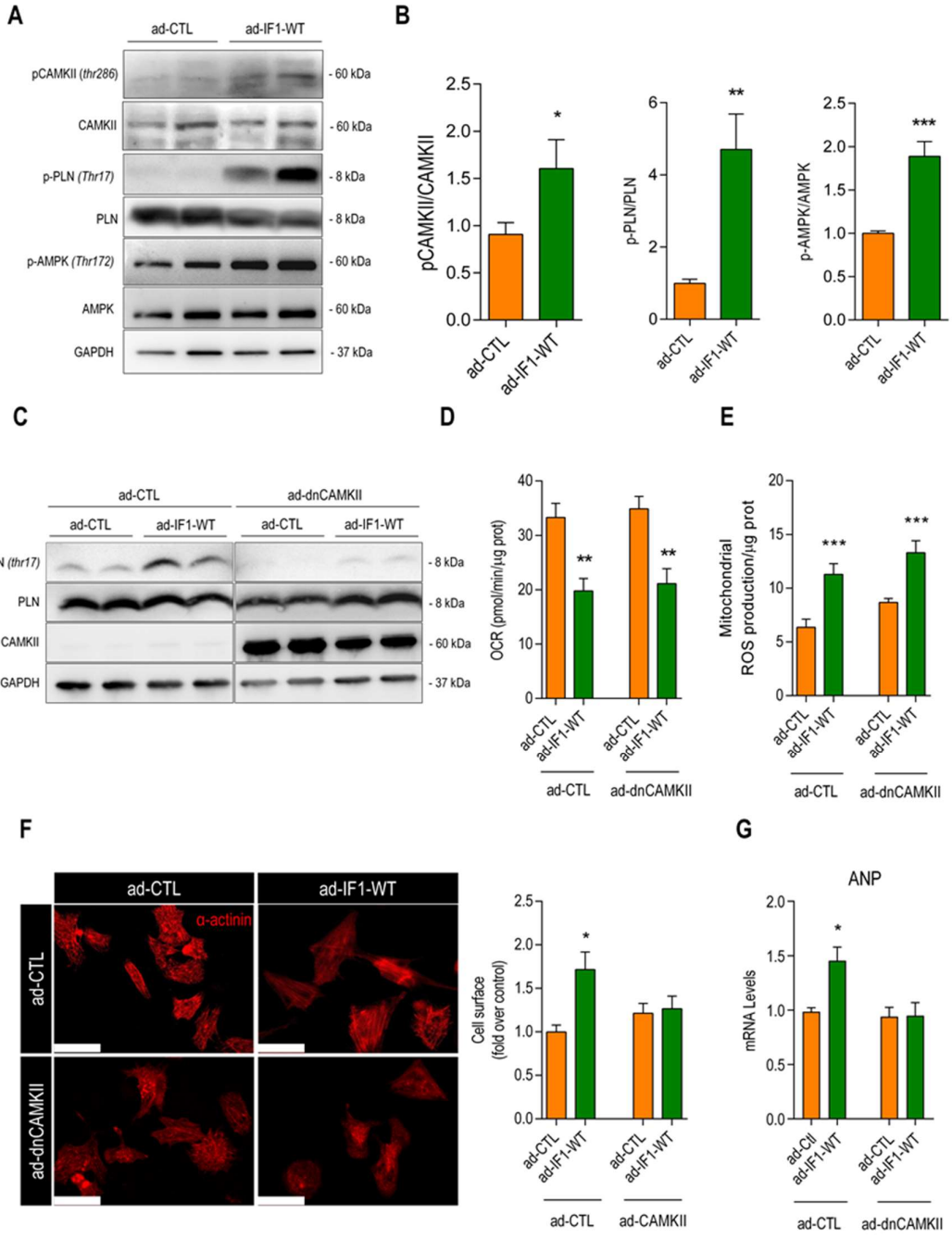

Preprints (www.preprints.org) | NOT PEER-REVIEWED | Posted: 26 March 2021 doi:10.20944/preprints202103.0655.v1

Figure 6. IF1-induced cardiomyocyte hypertrophy is dependent upon CaMKIIδ activation. *NRVMs were infected with adenovirus ad-IF1-WT and ad-CTL for 48 hrs.* ***(A)*** *Representative Immunoblot depicting phosphorylation of CAMKII (threonine 286) and CaMKII-dependent phosphorylation of phospholamban (threonine 17) and AMPK (threonine 172), normalized for the total protein (left panel).* ***(B)****, bar graphs depicting differences in phosphorylation between experimental groups (n=7).* ***(C)*** *NRVMs were co-infected with adenovirus expression IF1-WT or ad-CTL in the presence or absence of a catalytically dead mutant of CAMKIIδC (ad-dnCAMKII) for 48 hrs. Representative immunoblots from whole cell lysate using an antibody specific for p-PLN (thr17), total PLN, CAMKII (PAN) and GAPDH. (n=4).* ***(D)*** *Maximal mitochondria respiration through oxygen consumption rate (OCR) recorded using Mitostress test SeaHorse assay* ***(E)*** *Bar graph depicting basal mitochondrial ROS levels assayed with MitoSOX®. (n=4).* ***(F)*** *Typical example of immunofluorescent staining of cultured NRVMs with a fluorescent labelled anti-α-actinin (red, left panel) and (right panel) average cardiomyocyte surface area of α-actinin positive cells (scale bar represents 50 μm, n=4).* ***(G)*** *ANP mRNA level normalized for 36B4 (n=4). * Data are presented as mean ± SEM. *p < 0.05, **p < 0.01 and ***p < 0.001 vs ad-CTL using the Mann-Whitney U test* ***(A,B)*** *or the Kruskal-Wallis test* ***(D-G)****.*

IF1-induced cardiomyocyte hypertrophy is dependent upon CaMKII activation

To study the role of CaMKII activation in the pathological effects of IF1 described above, NRVMs were co-infected with an adenovirus expressing a catalytically dead mutant of the predominant cardiac isoform of CaMKII (CaMKIIδ; ad-dnCAMKII). As expected, infection with ad-dnCAMKII reduced CaMKII-dependent phosphorylation of PLN (**Figure 6C**). Co-infection with ad-dnCAMKII did not alter IF1-induced changes in maximal mitochondrial respiration (**Figure 6D**), nor did it affect mitochondrial ROS production (**Figure 6E**). Ad-dnCAMKII did, however, block IF1-induced cardiomyocyte hypertrophy (**Figure 6E**) and IF1-induced expression of ANP **(Figure 6F)**. Together these findings indicate that the effects of IF1 on cardiac hypertrophy are dependent on the activation of CaMKIIδ **(Figure 7)**.

Preprints (www.preprints.org) | NOT PEER-REVIEWED | Posted: 26 March 2021 doi:10.20944/preprints202103.0655.v1

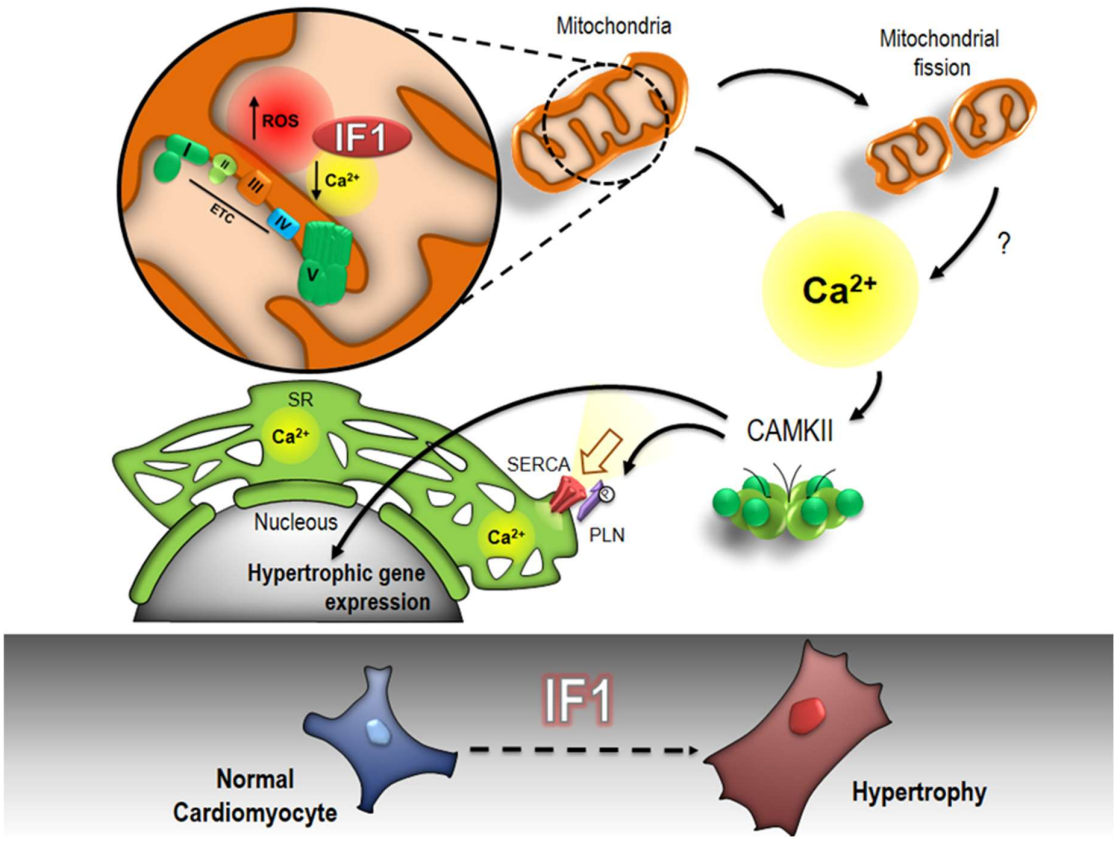

Figure 7. Schematic representation of the proposed mechanism responsible for IF1 mediated cardiomyocyte hypertrophy. *Under conditions of respiratory collapse, ATPase inhibitor factor-1 (IF1) prevents maladaptive ATP hydrolysis by ATP synthase (complex V). The function of IF1 under normal respiring conditions remains poorly described. We present evidence for a novel, ATP-synthase independent, role for IF1 in mitochondrial calcium handling and mitochondrial- to nuclear crosstalk involving Calcium-calmodulin Kinase II (CaMKII). Specifically, we found that IF1 induced mitochondrial oxidative stress, promoted mitochondrial fission and compromised mitochondrial calcium handling in primary cardiomyocytes. These perturbations resulted in sarcoplasmic reticulum calcium overload and the activation of CaMKII-mediated pathological cardiomyocyte hypertrophy. ETC, electron transport chain, ROS, reactive oxygen species, SERCA, Sarcoplasmic/endoplasmic reticulum calcium ATPase; PLN, phospholamban; SR, Sarcoplasmic Reticulum*

Discussion

 doi:10.20944/preprints202103.0655.v1

In the present study we investigated the role of IF1 in mitochondrial function and cardiomyocyte remodeling. Myocardial expression of IF1 was increased in mice and in humans with HF, downstream of neurohumoral signaling pathways, and in patterns that resembles the fetal-like gene program. Expression of IF1 in NRVMs induced metabolic changes that resembled the failing heart, including reductions in mitochondrial respiratory capacity, mitochondrial oxidative stress, and enhanced extra-mitochondrial glycolysis. Expression of IF1 alone was sufficient to induce pathological cardiomyocyte hypertrophy as evidenced by increases in cardiomyocyte size and expression of natriuretic peptides. The effects of IF1 on mitochondrial metabolism and cardiomyocyte hypertrophy occurred independent of ATP-synthase. Instead, IF1 promoted mitochondrial fragmentation and compromised mitochondrial Ca^{2+} handling through upregulation of MCUB. Together this resulted in reductions in mitochondrial Ca^{2+}, SR Ca^{2+} overloading and the cytosolic activation of CaMKIIδ. Finally, IF1 mediated cardiomyocyte hypertrophy was found to be depend on the activation of CaMKIIδ. Our findings suggest that IF1 represents a novel member of the fetal-like gene program that contributes to mitochondrial dysfunction and pathological cardiac remodeling in HF. Furthermore, we present evidence for a novel role for IF1 in mitochondrial Ca^{2+} handling and mitochondrial- to nuclear crosstalk involving CaMKIIδ.

The primary function of IF1 is to block the reverse mode of ATP-synthase, which can occur upon dissipation of the mitochondrial membrane potential under ischemic conditions or in critically damaged mitochondria[14]. By blocking ATP-synthase reversal, IF1 prevents mitochondria from becoming ATP consumers rather than generators. Under these conditions, IF1 also suppresses programmed cell death, and stimulates parkin-dependent elimination of dysfunctional mitochondria[8,9,15]. It has long been thought that the biological function of IF1 was restricted to conditions of respiratory compromise. However, several recent publications have suggested that IF1 can also inhibit the forward direction of ATP-synthase and thereby controls the rate of ATP synthesis under normal respiring conditions[6,16] Conversely, different research groups have rather demonstrated that IF1 promotes ATP synthase activity by stimulating mitochondrial cristae formation[8,9]. These conflicting results may reflect differences in cell types and experimental conditions, as most studies so far have been performed in immortalized cell lines and cancer models. In our hands, IF1 did not influence ATP-linked respiration and the structural and biochemical consequences of overexpression of IF1 also occurred with an IF1 mutant that is unable to bind to ATP-synthase. Our results therefore strongly suggest that the biological effects of IF1 under normal respiring conditions are independent of the canonical pathway that requires binding to ATP-synthase.

Preprints (www.preprints.org) | NOT PEER-REVIEWED | Posted: 26 March 2021 doi:10.20944/preprints202103.0655.v1

Overexpression of IF1 reduced maximal mitochondrial respiration and stimulated glycolysis. The reductions in mitochondrial respiratory capacity were associated with mitochondrial oxidative stress, significant damage to mitochondrial DNA and downregulation of mitochondrial respiratory chain complexes. In addition, IF1 stimulated mitochondrial fission and fragmentation, which by itself is sufficient to reduce mitochondrial respiration and promote oxidative stress [17]. IF1 has consistently been implicated in mitochondrial oxidative stress, yet the exact mechanism responsible remains enigmatic. Some authors have suggested that IF1-induced oxidative stress is caused by increased in the mitochondrial membrane potential, secondary to ATP-synthase inhibition [5]. However, our results clearly indicate that the mitochondrial oxidative stress induced by IF1 is independent on its capacity to bind to ATP-synthase. Further research is therefore required to determine the mechanisms of IF1-induced mitochondrial ROS.

The profound effects of IF1 on mitochondrial Ca^{2+} handling were, arguably, the most intriguing finding of our study. Overexpression of IF1 reduced the mitochondrial capacity to store Ca^{2+} and resulted in SR Ca^{2+} overloading. Aberrant SR Ca^{2+} handling is a central mechanism responsible for various pathophysiological changes in failing myocytes including but not restricted to cardiac arrythmia's, transcriptional activation of hypertrophy, mitochondrial dysfunction, and cell death [18]. IF1 could thus reflect a novel mechanistic link between mitochondrial dysfunction and dysregulated Ca^{2+} handling in HF. Our findings confirm and extend upon a recent study in which exogenous treatment with IF1 corresponded with increases in cytosolic Ca^{2+} levels in skeletal muscle cells [11]. The mechanisms responsible for IF1-induced reductions in mitochondrial Ca^{2+} are unknown, yet it is tempting to speculate that they rely on intrinsic biochemical properties of the IF1 molecule. For instance, it was recently discovered that Ca^{2+} influences the self-association and structure of IF1 and it is possible that IF1 influences the Ca^{2+} buffering in the mitochondrial matrix[19]. IF1 has also been shown to regulate critical Ca^{2+} handling proteins such as the MCU [7]. While we did not detect changes in the expression of MCU, IF1 did promote the expression of the negative regulator of MCU, MCUB. Finally, we cannot exclude the possibility that the reductions in mitochondrial Ca^{2+} were the consequence of mitochondrial oxidative stress or the mitochondrial fragmentation observed in our model. Nevertheless, our study contributes to the growing body of evidence that IF1 regulates mitochondrial Ca^{2+}.

IF1-induced SR Ca^{2+} overloading was associated with the activation of CaMKII and CaMKII-dependent induction of cardiomyocyte hypertrophy. Our results are in line with studies in global IF1 knock out mice, which appeared to be

Preprints (www.preprints.org) | NOT PEER-REVIEWED | Posted: 26 March 2021 doi:10.20944/preprints202103.0655.v1

protected from pressure overload-induced cardiomyocyte hypertrophy[14]. We confirm and extend upon these observations by providing a mechanistic link between SR Ca^{2+} overloading and the activation of CaMKIIδ. Multifunctional CaMKII has been implicated in a myriad of pathogenic cellular responses in HF, which include mitochondrial reprograming, mitochondrial oxidative stress and mitochondrial fragmentation[20-22]. Nevertheless, IF1-induced reductions in mitochondrial respiration and mitochondrial ROS were not affected by catalytically dead CaMKIIδ. The activation of CaMKIIδ thus appears to be a consequence of IF1-induced mitochondrial dysfunction rather than a cause. Of note, CaMKIIδ can also be activated by ROS and we cannot determine whether the activation of CaMKIIδ in our model was dependent upon Ca^{2+} or ROS.

While our study provides compelling evidence for a role of IF1 in controlling mitochondrial oxidative stress and mitochondrial Ca^{2+} homeostasis in cardiomyocytes, several limitations need to be acknowledged. One of the main limitations of our experimental model is that neonatal cardiomyocytes display a relatively immature metabolic phenotype that is highly glycolytic. Therefore, the role of IF1 on mitochondrial metabolism may be different in adult cardiomyocytes or *in vivo*. Moreover, ATP-linked respiration is modest in NRVMs, which may have prevented us from detecting subtle changes in ATP-lined respirations induced by IF1. Nevertheless, studies with the ad-IF1-E55A mutant clearly demonstrated that neither the metabolic, nor the structural changes induced by IF1 were dependent on binding of IF1 to ATP-synthase. Another limitation of our study is that we do not provide mechanisms responsible for IF1-induced mitochondrial oxidative stress and mitochondrial fission since, to our opinion, this is beyond the scope of the current investigation.

Based on our results we suggest that the increase in the expression of IF1 in HF is maladaptive and contributes to mitochondrial fragmentation, aberrant Ca2+ handling and CAMKIIδ-dependent pathological remodeling. Our study reinforces the concept that mitochondrial dysfunction has profound effects in failing cardiomyocytes that extend beyond bioenergetic insufficiency. Finally, the present work underscores a central role of mitochondria in pathological growth responses in the heart and supports current efforts to design mitochondrial targeted therapies for HF [23,24].

Conclusion

Preprints (www.preprints.org) | NOT PEER-REVIEWED | Posted: 26 March 2021 doi:10.20944/preprints202103.0655.v1

IF1 represents a novel member of the fetal-like gene program that contributes to mitochondrial dysfunction and pathological cardiac remodeling in HF. Furthermore, we present evidence for a novel, ATP-synthase independent, role for IF1 in mitochondrial Ca^{2+} handling and mitochondrial- to nuclear crosstalk involving CaMKII.

Material and Methods

The use of animals for these studies was in accordance with the National Institutes of Health *Guide for the Care and Use of Laboratory Animals*. The studies were submitted to and approved by the Institutional Animal Care and Use Committee of the University of Groningen or the University of California San Diego.

Heart failure samples

mRNA was isolated from viable left ventricular tissue from 3 different murine models for chronic heart failure; first, Gαq-40 transgenic mice has been described previously [25]. Second, transverse aortic constriction (TAC) was performed with a 7–0 nylon suture between the carotid arteries around a 27G needle, as described [26]. Third, post-myocardial infarction (MI) heart failure was achieved through a permanent ligation of the left coronary artery with a Premilene 6–0 suture [26]. Human myocardial tissue was obtained from patients with end-stage ischemic heart failure (n=10) and from donor hearts rejected due to technical reasons (n=19) within the heart transplant program at the Heart- und Diabetes Center NRW. The study was approved by the local ethical committee and conducted in accordance with the guidelines in the Declaration of Helsinki.

Neonatal rat cardiomyocytes isolation

The use of animals for these studies was in accordance with the National Institutes of Health *Guide for the Care and Use of Laboratory Animals*. The study was submitted to and approved by the Committee for Animal Experiments of the University of Groningen. Euthanasia was performed by quick decapitation. Primary neonatal rat ventricular cardiomyocytes (NRVMs) were isolated from neonatal rats of 1–2 days old, as previously described[27]. NRVMs were grown in MEM (Sigma M1018) supplemented with 5% fetal bovine serum (FBS) (Thermo Fisher SV30160) and penicillin-streptomycin (100 U/ml-100

Preprints (www.preprints.org) | NOT PEER-REVIEWED | Posted: 26 March 2021 doi:10.20944/preprints202103.0655.v1

µg/ml) (Thermo Fisher 15070063). IF1 wild-type sequence (IF1-WT) was cloned into adenovirus pSF-Ad5-WT OG617 using the E1A promoter (Oxford Genetics). Inactive form of IF1 (E55A) sequence was cloned previously by Prof. David Sabatini (Addgene #85404) [28]. NRVMs were infected with recombinant adenovirus particles [multiplicity of infection (MOI) 50- 300] 24h after isolation and 1% FBS in DMEM with penicillin-streptomycin (100 U/ml-100 µg/ml) the day after.

Biochemical analysis

Western blot

SDS-PAGE assays were performed by separating 10-20 µg of protein after cell lysis with RIPA buffer plus protease inhibitor (Roche 11873580001), phosphatase inhibitor cocktail 3 (Sigma P2850:), sodium orthovanadate (Sigma S6508) and phenylmethylsulfonyl fluoride (PMSF) (Roche 10837091001). Protein quantification was measured with BCA assay (Pierce 23225). The samples were incubated with 5x loading buffer (final 10% glycerol (Sigma G5516), 2%SDS (Fluka 05030), 0,3% DTT (Sigma 43819), 66 mM Tris (Sigma T6066) and bromophenol blue (Sigma 114391) and cocked at 95 C. For OXPHOS (Abcam ab110413) detection, the samples were incubated with sample buffer and warmed at 37 C. After electrophoresis, proteins were transferred to PVDF membranes (BioRad 162-0177). Membranes were blocked and incubated with primary and secondary-HRP labelled antibodies (Dako) before detection with chemiluminescence (ECL) (PerkinElmer NEL112001EA). The specific primary and secondary antibodies that were used are depicted in **table S1.**

Real time PCR

To analyze gene expression, total RNA was isolated using TRI reagent according to the protocol provided (Sigma, T9424). RNA concentrations have been determined with a Nanodrop 2000 (Thermo Scientific) and cDNA was synthetized by reverse transcription using QuantiTect Reverse Transcription Kit (Qiagen 205313) and real time qPCR were performed with IQ SYBR green (BioRad 170-8885) using specific primers (see table 1). Relative expression levels were calculated using $2^{(-\Delta\Delta CT)}$.

To assess mitochondrial DNA to nuclear DNA ratio and DNA damage, Total DNA including mtDNA was extracted from the non-infarcted left ventricle using Nucleospin Tissue XS (Macherey-Nagel 740.901.50). mtDNA-to-nDNA ratio was determined by quantitative real-time polymerase chain reaction (qRT-PCR), as described previously [29]. Mitochondrial DNA copies were corrected for nuclear DNA values, and the calculated values were expressed relative to the control group

Preprints (www.preprints.org) | NOT PEER-REVIEWED | Posted: 26 March 2021 doi:10.20944/preprints202103.0655.v1

per experiment. To determine DNA damage (lesions/10 kb), two protocols for RT-QPCR were performed. Firstly, a short mitochondrial DNA fragment was amplified with a short-run protocol. Secondly, a long mitochondrial DNA fragment was amplified with a long-run protocol. The D-loop mitochondrial genomic region was amplified by a semi-long-run qRT-PCR. A list of primer sequences used for this manuscript is listed in the online data supplement (**table S2**).

Mitochondrial membrane potential

For mitochondrial potential measurements, the cells were plated in individual petridishes with glass bottom FluoroDish Cell Culture Dish - 35mm (WPI FD35-100). Tetramethylrhodamine (TMRE; 100 nM; ThermoFisher T669,) was added to the culture media and incubated for 30 minutes at 37°C, 5% CO_2. Hereafter, the cells were washed 3 times with Krebs buffer and maintained in this medium at room temperature for the rest of the experiment. A time-lapse series (200 pictures in 12 minutes) was made using a Leica AF-6000 epifluorescence microscope. After 1 minute of base line measurements, Rotenone (4 µM) (Sigma R8875) and Antimycin-A (2 µM) (Sigma A8674) dissolved in Krebs buffer and added to the medium. One minute before the end of the time-lapse, FCCP (20 µM) (Enzo BML-CM120-0010) was added. Imaging analyses was performed using ImageJ.

ATP measurements

ATP concentrations were measured in whole cell lysates using an ATP Assay Kit (colorimetric/fluorometric) from Abcam (#ab83355, Cambridge, UK) according to the manufacturer's instructions. Results are normalized for protein concentration.

Seahorse assays

Measuring oxygen consumption rate (OCR) and extracellular acidification rate (ECAR) were performed using the Agilent Seahorse Bioscience XF96 analyzer. Briefly, 80,000 cells/well previously treated with specific adenoviruses were cultured in 96-well culture plates (Agilent 100850-001) using the XF MitoStress and XF GlycoStress protocol, according to the guidelines provided by the supplier (Agilent Technologies). Every condition was simultaneously measured in at least 8 wells per experiment. Results were normalized to protein levels detected with the BCA method performed at the end of the experiment. Data were obtained using Wave software.

Mitochondrial morphology

Preprints (www.preprints.org) | NOT PEER-REVIEWED | Posted: 26 March 2021 doi:10.20944/preprints202103.0655.v1

Cells were plated on glass coverslips and stained with Mitotracker deep red (200 nM) for 30 min (Invitrogen M22426). Immediately after mitochondrial stain cells were washed 3 times in PBS 1X and fixed with PFA 4% and processed as described in the cell size section. FITC-labelled α-actinin (Sigma A7811) was employed as a marker for cardiomyocytes. Image acquisition was performed using Leica Sp8 Lightning confocal microscope. Z-stacks was obtained from two independent channels and imaging deconvolution were performed using Huygens Pro. Processed image were analyzed by Imaris software. Cell surface was measured, and 3D reconstruction was performed by surface area detailed level (0.2 μM) from red (mitochondria) and green channel (α-actinin) respectively. Number of particle and total mitochondrial volume was quantified per cell.

Mitochondrial and cytosolic Ca2+ levels

For Mitochondrial Ca2+ content/release, the cells were plated in individual petridishes with glass bottom: FluoroDish Cell Culture Dish - 35mm (WPI FD35-100). Both Ca^{2+} label were used for the measurement mitochondrial Ca2+ content: Rhod2-AM and Fluo4-AM (5 μM; ThermoFisher F14201). Thapsigargin (10 μM; Enzo BML-PE180-001;) were added to the culture media and incubated for 30 minutes at 37°C, 5% CO_2. Hereafter, the cells were washed 3 times with Ca^{2+}-free Krebs buffer. A time-lapse (200 pictures in 30 minutes) was made using with a Leica AF-6000 microscope. After 2 minutes, FCCP (20 μM) suspended in Ca^{2+}-free Krebs buffer was added. Imaging analyse was performed using ImageJ.

For cytosolic Ca2+ measurement, the cells were plated in individual petridishes with glass bottoms (35mm). FURA 2-AM (4 μM; Abcam ab120873;) was added to the culture medium and incubated for 45 minutes at 37°C, 5% CO_2. Hereafter, the cells were washed 3 times with Ca^{2+}-free Krebs buffer. A time-lapse of 5 min was measured with 340 and 380nm wavelength using Leica DM IRE2 and Polychorome V (Till photonics). After 1 minute, KCL (50 mM) suspended in Ca^{2+}-free Krebs buffer was added. The ratio of 340/380 wavelength fluorescence analysis was performed using ImageJ.

Cell size

For cell-size measurement, cells were cultured on laminin (Millipore CC095)-coated coverslips for 48h, and then transfected with the specific adenoviruses. The cardiomyocytes were fixed with 4% paraformaldehyde (Merck 4005) in phosphate buffer for 5 minutes at room temperature. After, the cells were washed in PBS 1x and followed by permeabilization with PBS + 0.3% Triton-X100 (Sigma-Aldrich, T9284) on ice for 5 minutes. For images acquisition we used Leica SP8 epifluorescence microscopy (Leica, Germany) and for the analysis we used ImageJ software (NIH, Bethesda, MD, USA) for the determination of cellular area. Five observation fields were selected randomly on each cover slip, and

5-10 cells within each observation field were selected for the determination of the mean cardiomyocyte surface area according to the image analysis system. For the measurements, we used at least 5 different fields from 5 independent cultures in each condition (>50 cells).

Statistical analysis

All data are presented as mean ± SEM. Comparisons between groups were performed using the Student *t* test, the Mann–Whitney *U* test, Kruskal–Wallis test, or 1-way ANOVA, followed by the Tukey post hoc test, where appropriate. A *P* value <0.05 was considered statistically significant.

Acknowledgments

We acknowledge Dr. John Walker (MRC Mitochondrial Biology unit, University of Cambridge, Cambridge, United Kingdom) for his support and expert advice throughout this study. We thank Dr Walter W. Chen and Dr. David M. Sabatini (Whitehead Institute for Biomedical Research, Cambridge, MA, USA) for providing us with the IF1 plasmids. We thank Marloes Schouten, Martin Dokter and Janny Takens for expert technical assistance and advice.

References

1. Brown, D.A.; Perry, J.B.; Allen, M.E.; Sabbah, H.N.; Stauffer, B.L.; Shaikh, S.R.; Cleland, J.G.; Colucci, W.S.; Butler, J.; Voors, A.A.; et al. Expert consensus document: Mitochondrial function as a therapeutic target in heart failure. *Nature reviews. Cardiology* **2017**, *14*, 238-250, doi:10.1038/nrcardio.2016.203.

2. Tian, R.; Colucci, W.S.; Arany, Z.; Bachschmid, M.M.; Ballinger, S.W.; Boudina, S.; Bruce, J.E.; Busija, D.W.; Dikalov, S.; Dorn, G.W., II; et al. Unlocking the Secrets of Mitochondria in the Cardiovascular System: Path to a Cure in Heart Failure-A Report from the 2018 National Heart, Lung, and Blood Institute Workshop. *Circulation* **2019**, *140*, 1205-1216, doi:10.1161/CIRCULATIONAHA.119.040551.

3. Feniouk, B.A.; Yoshida, M. Regulatory mechanisms of proton-translocating F(O)F (1)-ATP synthase. *Results and problems in cell differentiation* **2008**, *45*, 279-308, doi:10.1007/400_2007_043.

4. Cabezon, E.; Montgomery, M.G.; Leslie, A.G.; Walker, J.E. The structure of bovine F1-ATPase in complex with its regulatory protein IF1. *Nature structural biology* **2003**, *10*, 744-750, doi:10.1038/nsb966.

5. Formentini, L.; Sanchez-Arago, M.; Sanchez-Cenizo, L.; Cuezva, J.M. The mitochondrial ATPase inhibitory factor 1 triggers a ROS-mediated retrograde prosurvival and proliferative response. *Molecular cell* **2012**, *45*, 731-742, doi:10.1016/j.molcel.2012.01.008.

6. Garcia-Aguilar, A.; Cuezva, J.M. A Review of the Inhibition of the Mitochondrial ATP Synthase by IF1 in vivo: Reprogramming Energy Metabolism and Inducing Mitohormesis. *Frontiers in physiology* **2018**, *9*, 1322, doi:10.3389/fphys.2018.01322.

7. Faccenda, D.; Gorini, G.; Jones, A.; Thornton, C.; Baracca, A.; Solaini, G.; Campanella, M. The ATPase Inhibitory Factor 1 (IF1) regulates the expression of the mitochondrial Ca(2+) uniporter (MCU) via the AMPK/CREB pathway. *Biochimica et biophysica acta. Molecular cell research* **2020**, *1868*, 118860, doi:10.1016/j.bbamcr.2020.118860.

8. Campanella, M.; Casswell, E.; Chong, S.; Farah, Z.; Wieckowski, M.R.; Abramov, A.Y.; Tinker, A.; Duchen, M.R. Regulation of mitochondrial structure and function by the F1Fo-ATPase inhibitor protein, IF1. *Cell metabolism* **2008**, *8*, 13-25, doi:10.1016/j.cmet.2008.06.001.

9. Faccenda, D.; Nakamura, J.; Gorini, G.; Dhoot, G.K.; Piacentini, M.; Yoshida, M.; Campanella, M. Control of Mitochondrial Remodeling by the ATPase Inhibitory Factor 1 Unveils a Pro-survival Relay via OPA1. *Cell reports* **2017**, *18*, 1869-1883, doi:10.1016/j.celrep.2017.01.070.

10. Formentini, L.; Pereira, M.P.; Sanchez-Cenizo, L.; Santacatterina, F.; Lucas, J.J.; Navarro, C.; Martinez-Serrano, A.; Cuezva, J.M. In vivo inhibition of the mitochondrial H+-ATP synthase in neurons promotes metabolic preconditioning. *The EMBO journal* **2014**, *33*, 762-778, doi:10.1002/embj.201386392.

11. Lee, H.J.; Moon, J.; Chung, I.; Chung, J.H.; Park, C.; Lee, J.O.; Han, J.A.; Kang, M.J.; Yoo, E.H.; Kwak, S.Y.; et al. ATP synthase inhibitory factor 1 (IF1), a novel myokine, regulates glucose metabolism by AMPK and Akt dual pathways. *FASEB journal : official publication of the Federation of American Societies for Experimental Biology* **2019**, *33*, 14825-14840, doi:10.1096/fj.201901440RR.

12. Fernandez-Cardenas, L.P.; Villanueva-Chimal, E.; Salinas, L.S.; Jose-Nunez, C.; Tuena de Gomez Puyou, M.; Navarro, R.E. Caenorhabditis elegans ATPase inhibitor factor 1 (IF1) MAI-2 preserves the mitochondrial membrane potential (Deltapsim) and is important to induce germ cell apoptosis. *PloS one* **2017**, *12*, e0181984, doi:10.1371/journal.pone.0181984.

13. Martin-Jimenez, R.; Faccenda, D.; Allen, E.; Reichel, H.B.; Arcos, L.; Ferraina, C.; Strobbe, D.; Russell, C.; Campanella, M. Reduction of the ATPase inhibitory factor 1 (IF1) leads to visual impairment in vertebrates. *Cell death & disease* **2018**, *9*, 669, doi:10.1038/s41419-018-0578-x.

14. Yang, K.; Long, Q.; Saja, K.; Huang, F.; Pogwizd, S.M.; Zhou, L.; Yoshida, M.; Yang, Q. Knockout of the ATPase inhibitory factor 1 protects the heart from pressure overload-induced cardiac hypertrophy. *Scientific reports* **2017**, *7*, 10501, doi:10.1038/s41598-017-11251-8.

15. Hoshino, A.; Wang, W.J.; Wada, S.; McDermott-Roe, C.; Evans, C.S.; Gosis, B.; Morley, M.P.; Rathi, K.S.; Li, J.; Li, K.; et al. The ADP/ATP translocase drives mitophagy independent of nucleotide exchange. *Nature* **2019**, *575*, 375-379, doi:10.1038/s41586-019-1667-4.

16. Garcia-Bermudez, J.; Sanchez-Arago, M.; Soldevilla, B.; Del Arco, A.; Nuevo-Tapioles, C.; Cuezva, J.M. PKA Phosphorylates the ATPase Inhibitory Factor 1 and Inactivates Its Capacity to Bind and Inhibit the Mitochondrial H(+)-ATP Synthase. *Cell reports* **2015**, *12*, 2143-2155, doi:10.1016/j.celrep.2015.08.052.

17. Giacomello, M.; Pyakurel, A.; Glytsou, C.; Scorrano, L. The cell biology of mitochondrial membrane dynamics. *Nature reviews. Molecular cell biology* **2020**, doi:10.1038/s41580-020-0210-7.

18. Braunwald, E. The war against heart failure: the Lancet lecture. *Lancet* **2015**, *385*, 812-824, doi:10.1016/S0140-6736(14)61889-4.

19. Boreikaite, V.; Wicky, B.I.M.; Watt, I.N.; Clarke, J.; Walker, J.E. Extrinsic conditions influence the self-association and structure of IF1, the regulatory protein of mitochondrial ATP synthase. *Proceedings of the National Academy of Sciences of the United States of America* **2019**, *116*, 10354-10359, doi:10.1073/pnas.1903535116.

20. Mattiazzi, A.; Bassani, R.A.; Escobar, A.L.; Palomeque, J.; Valverde, C.A.; Vila Petroff, M.; Bers, D.M. Chasing cardiac physiology and pathology down the CaMKII cascade. *American journal of physiology. Heart and circulatory physiology* **2015**, *308*, H1177-1191, doi:10.1152/ajpheart.00007.2015.

21. Westenbrink, B.D.; Edwards, A.G.; McCulloch, A.D.; Brown, J.H. The promise of CaMKII inhibition for heart disease: preventing heart failure and arrhythmias. *Expert opinion on therapeutic targets* **2013**, *17*, 889-903, doi:10.1517/14728222.2013.809064.

22. Xu, S.; Wang, P.; Zhang, H.; Gong, G.; Gutierrez Cortes, N.; Zhu, W.; Yoon, Y.; Tian, R.; Wang, W. CaMKII induces permeability transition through Drp1 phosphorylation during chronic beta-AR stimulation. *Nature communications* **2016**, *7*, 13189, doi:10.1038/ncomms13189.

23. Butler, J.; Khan, M.S.; Anker, S.D.; Fonarow, G.C.; Kim, R.J.; Nodari, S.; O'Connor, C.M.; Pieske, B.; Pieske-Kraigher, E.; Sabbah, H.N.; et al. Effects of Elamipretide on Left Ventricular Function in Patients with Heart Failure with Reduced Ejection Fraction: The PROGRESS-HF Phase 2 Trial. *Journal of cardiac failure* **2020**, doi:10.1016/j.cardfail.2020.02.001.

24. Yurista, S.R.; Sillje, H.H.W.; Oberdorf-Maass, S.U.; Schouten, E.M.; Pavez Giani, M.G.; Hillebrands, J.L.; van Goor, H.; van Veldhuisen, D.J.; de Boer, R.A.; Westenbrink, B.D. Sodium-glucose co-transporter 2 inhibition with empagliflozin improves cardiac function in non-diabetic rats with left ventricular dysfunction after myocardial infarction. *European journal of heart failure* **2019**, *21*, 862-873, doi:10.1002/ejhf.1473.

25. Westenbrink, B.D.; Ling, H.; Divakaruni, A.S.; Gray, C.B.; Zambon, A.C.; Dalton, N.D.; Peterson, K.L.; Gu, Y.; Matkovich, S.J.; Murphy, A.N.; et al. Mitochondrial reprogramming induced by CaMKIIdelta mediates hypertrophy decompensation. *Circulation research* **2015**, *116*, e28-39, doi:10.1161/CIRCRESAHA.116.304682.

26. Booij, H.G.; Yu, H.; De Boer, R.A.; van de Kolk, C.W.; van de Sluis, B.; Van Deursen, J.M.; Van Gilst, W.H.; Sillje, H.H.; Westenbrink, B.D. Overexpression of A kinase interacting protein 1 attenuates myocardial ischaemia/reperfusion injury but does not influence heart failure development. *Cardiovascular research* **2016**, *111*, 217-226, doi:10.1093/cvr/cvw161.

27. Tigchelaar, W.; de Jong, A.M.; Bloks, V.W.; van Gilst, W.H.; de Boer, R.A.; Sillje, H.H. Hypertrophy induced KIF5B controls mitochondrial localization and function in neonatal rat cardiomyocytes. *Journal of molecular and cellular cardiology* **2016**, *97*, 70-81, doi:10.1016/j.yjmcc.2016.04.005.

28. Chen, W.W.; Birsoy, K.; Mihaylova, M.M.; Snitkin, H.; Stasinski, I.; Yucel, B.; Bayraktar, E.C.; Carette, J.E.; Clish, C.B.; Brummelkamp, T.R.; et al. Inhibition of ATPIF1 ameliorates severe mitochondrial respiratory chain dysfunction in mammalian cells. *Cell reports* **2014**, *7*, 27-34, doi:10.1016/j.celrep.2014.02.046.

29. Tigchelaar, W.; De Jong, A.M.; van Gilst, W.H.; De Boer, R.A.; Sillje, H.H. In EXOG-depleted cardiomyocytes cell death is marked by a decreased mitochondrial reserve capacity of the electron transport chain. *BioEssays : news and reviews in molecular, cellular and developmental biology* **2016**, *38 Suppl 1*, S136-145, doi:10.1002/bies.201670914.

.

Supplementary Materials: The following are available online Table S1-S7: Table S1-S2

Funding sources

P.v.M. is supported by European Research Council (grant: ERC-2016-StG – 715732). R.A.d.B is supported by the Netherlands Heart Foundation (CVON DOSIS, grant 2014-40, CVON SHE-PREDICTS-HF, grant 2017-21, and CVON RED-CVD, grant 2017-11) and the CVON DOUBLE DOSE grant (grant 2020-8005); and the Innovational Research Incentives Scheme program of the Netherlands Organization for Scientific Research (NWO VIDI, grant 917.13.350). S.M. is supported by the American Heart Association (19TPA34910011) J.H.B. is supported by the National Heart, Lung, and Blood Institute (R37-HL-028143, and R01-HL-145459) and. B.D.W is supported by The Netherlands Organization for

Scientific Research (NWO VENI, grant 016.176.147), the Netherlands Heart Foundation Senior Clinical Scientist Grant (2019T064) and CVON DOUBLE DOSE (grant 2020-8005).

Author contribution statement

Conceived and designed the study: M.P.G. and B.D.W.

Performed the experiments: M.P.G., P.S.A, N.B., H.G.B., P.G., S.R.Y, S.O.M., K.T.N.

Analyzed the data: M.P.G., P.S.A., N.B., P.S.A, H.G.B., P.G., K.T.N.

Contributed protocols/reagents/materials/analysis tools: All authors

Drafting the manuscript: M.P.G., N.B., and B.D.W.

Critically reviewed the manuscript: All authors

Final Approval: All authors

Disclosures

M.P.G., N.B., H.G.B., P.G., S.M.O., K.T.N., S.M., S.R.Y., P.vd.M., J.H.B., H.H.W.S., and B.D.W. do not report conflicts of interest relative to this report. The UMCG, which employs M.P.G, N.B., H.G.B., P.G., S.O.M, K.T.N., S.R.Y., P.vd.M., H.H.W.S., and B.D.W. has received research grants and/or fees from Abbott, AstraZeneca, Bristol-Myers Squibb, Novartis, Novo Nordisk, and Roche. R.A.d.B. received personal fees from Abbott, AstraZeneca, Novartis. J.C.N.

Institutional Review Board Statement: The use of animals for these studies was in accordance with the National Institutes of Health *Guide for the Care and Use of Laboratory Animals*. The studies were submitted to and approved by the Institutional Animal Care and Use Committee of the University of Groningen or the University of California San Diego. The collection and analysis of human samples was approved by the local ethical committee and conducted in accordance with the guidelines in the Declaration of Helsinki.